

Fig. 3 Ratio of average to peak velocities at duct exit vs area ratio. Combinations of n and ϕ' are such as to keep $f_1' = 0.9 = \text{const}$.

Sovran¹ showed that $f_1'' (= E_2$ in his notation) correlates closely with a quantity defined as $\alpha(100B_1)^{1/4}$ and presents a single empirical curve which correlates well with a large amount of data on conical diffusers. The correlation is expected to hold for diffusers whose area ratio is such that C_p is maximum for a given length/diameter ratio ("optimum" diffusers). Such diffusers are relatively loss-free and are hence most likely to agree with an inviscid theory.

The two dashed lines of Fig. 2 have been calculated from Sovran's correlation (Fig. 22 of Ref. 1). They are to be compared with the top two curves of the family drawn in continuous lines, representing the present results.

The general trends in terms of both α and f_1' are in agreement with the empirical correlation, the measured exit blockage values being greater than the predicted ones. The worst deviation in f_1'' is 0.16, which is roughly twice as much as the data scatter around the correlation curve. Since Sovran's correlation is not claimed to hold for $f_1' \leq 0.9$, no comparison curves were drawn for lower values.

The comparison of theoretical and empirical results is shown in Fig. 2 only for the arbitrarily chosen exponent of $n = 1.5$. If our postulate that f_1' is adequate to characterize the inlet profile is correct then the choice of n should be irrelevant. This means that the $f_1''(\alpha)$ function should be independent of n . Figure 3 shows that the effect of n (as predicted by this theory) is indeed very weak. Figure 3 refers to $f_1' = 0.9$ only, but other values yield similar plots.

The curves of Fig. 3 are discontinued when ϕ'' reaches unity. The area ratio at which such a "separation" occurs depends strongly on n . This trend is probably not realistic because the location of separation is strongly influenced by the neglected viscous effects.

Our second major assumption concerning the power law shape of the velocity profiles at all stations is tested by comparing present predictions against numerical solutions of the equation

$$\nabla^2 \psi = -\omega(\psi) \quad (13)$$

where ψ is the stream function and ω is the vorticity whose dependence on ψ is given through the specification of the inlet velocity profile. The lateral velocity components were assumed zero at the inlet station and the static pressure was assumed constant over the exit plane. The computer program, based on a line relaxation scheme, is from Hoffman.² Conical diffuser shapes were used, preceded and followed by three diameter long constant area pipes.

Each diamond in Figs. 1 and 2 represents one such complete flowfield computation. Each is to be compared with the continuous line lying nearest to it. The agreement is clearly very good, indicating that the restriction placed on profile shapes is much less important than the neglect of viscosity.

It is concluded that the presented formulae may be useful for estimation purposes and for describing some velocity profile effects in short, unstalled ducts where pressure forces are dominant.

References

- ¹ Sovran, G. and Klomp, E. D., "Experimentally Determined Optimum Geometries for Rectilinear Diffusers with Rectangular, Conical or Annular Cross Section," *Fluid Mechanics of Internal Flow*, Elsevier, New York, 1967, pp. 270-319.
- ² Hoffman, G. H., "Rotational Inviscid Flow in Axisymmetric Ducts," Rept. MDC Q0472, 1973, McDonnell Douglas Research Labs., St. Louis, Mo.

A Note on the Shock Standoff Distance for a Spherical Body in Supersonic Flow

T. B. GUY*

Australian Atomic Energy Commission, Lucas Heights,
N.S.W., Australia

THE object of this Note is to introduce a simple approximate method of estimating the distance a shock wave stands ahead of a spherical body in supersonic flow. The method assumes that the shock wave is sufficiently close to the body and that it can be considered to be spherical in the neighborhood of the normal in the direction of flow. It is further assumed that the pressure and Mach number conditions shown in the coordinate system in Fig. 1 are precisely those which would apply if the shock wave were produced as a result of an outward-going shock wave undergoing spherical diffraction.

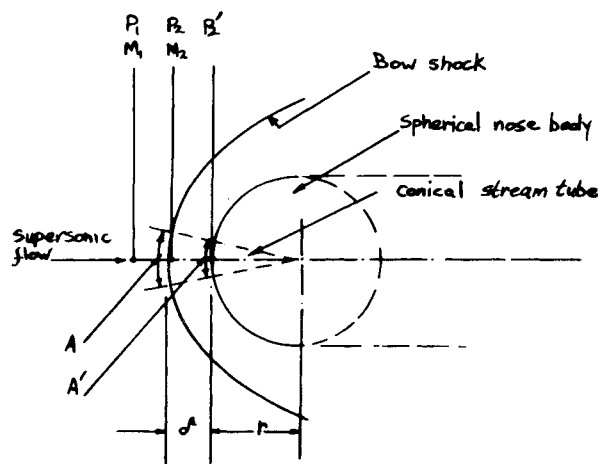


Fig. 1 Sketch of bow shock and spherical body with notation.

With these assumptions, we use the shock strength to ray tube area relationships given by Chisnall¹ as

$$(A/A')^{K_{(Z)}} = (Z_2' - 1)/(Z_2 - 1) \quad (1)$$

where $K_{(Z)}$, plotted in Fig. 2, is given by Whitham² as

$$K_{(Z)} = 2 \left[\frac{1 + 2(1 - \mu^2)}{(\gamma + 1)} \right] \left\{ 2\mu + 1 + \frac{2\gamma}{(\gamma - 1) + (\gamma + 1)Z} \right\}^{-1} \quad (2)$$

with

$$\mu^2 = [(\gamma + 1) + (\gamma - 1)Z]/2\gamma Z$$

Received May 24, 1973, revision received October 2, 1973.

Index categories: Supersonic and Hypersonic Flow; Shock Waves and Detonations.

* Engineering Research Division.

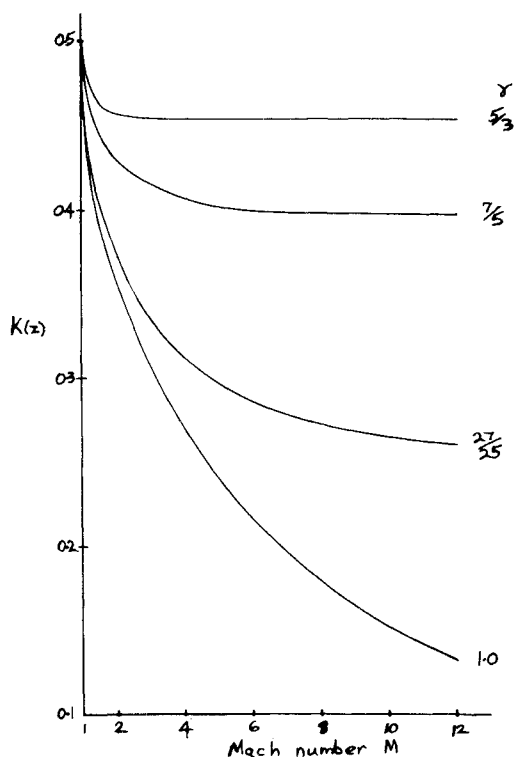


Fig. 2 Variation in $K(z)$ with Mach number for the range $\gamma = \frac{5}{3}$ to $\gamma = 1.0$.

For the spherical case under consideration, Eq. (1) becomes

$$[(r+\delta)/r]^{2K(z)} = (Z_2' - 1)/(Z_2 - 1) \quad (3)$$

where

$$Z_2 = [2\gamma M_1^2 - (\gamma - 1)]/(\gamma + 1) \quad (4)$$

$$Z_2' = Z_2[1 + \gamma M_2^2/2] \quad (5)$$

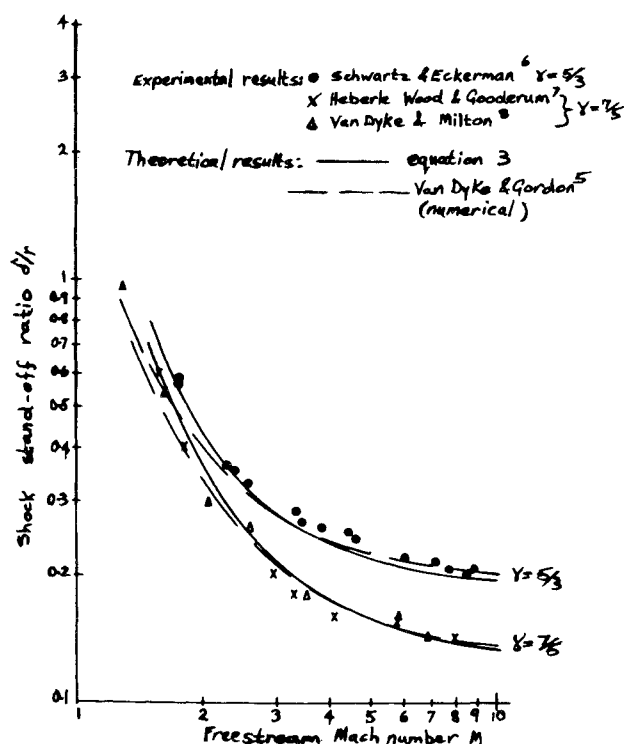


Fig. 3 Comparison between theoretical and experimental variation in δ/r with M for $\gamma = \frac{5}{3}$ and $\gamma = \frac{7}{5}$.

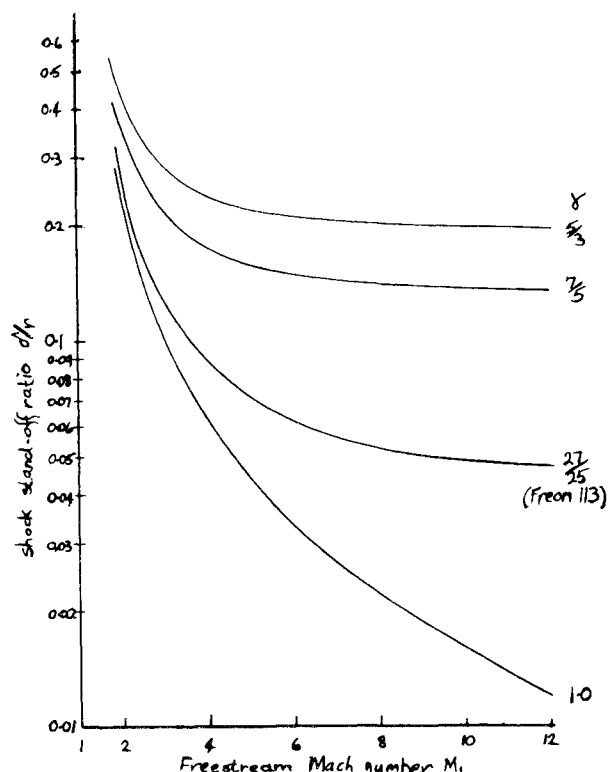


Fig. 4 Theoretical shock stand-off ratio with freestream Mach number for the γ range $\frac{5}{3}$ to 1.0.

$$M_2^2 = [(\gamma - 1)M_1^2 + 2]/[2\gamma M_1^2 - (\gamma - 1)] \quad (6)$$

in which case Eq. (3) reduces to

$$\frac{\delta}{r} = \left[\left\{ \frac{(\gamma - 1)M_1^2 + 2}{4(M_1^2 - 1)} + 1 \right\}^{1/2K(z)} - 1 \right] \quad (7)$$

The shock stand-off ratio δ/r calculated as a function of free-stream Mach number using Eq. (7) is shown in Fig. 3 for values of $\gamma = \frac{5}{3}$ and $\frac{7}{5}$. These results are compared with the experimental results of Schwartz and Eckerman³ for $\gamma = \frac{5}{3}$ and to the results of Heberle, Wood, and Gooderum⁴ and Van Dyke and Milton⁵ for $\gamma = \frac{7}{5}$. The numerical results of Van Dyke and Gordon⁶ for $\gamma = \frac{5}{3}$ and $\frac{7}{5}$ are also included in Fig. 3. Finally the spread of stand-off distance with Mach number in gases having different values of γ , calculated from Eq. (7), is shown in Fig. 4 which includes the hypothetical value $\gamma = 1$.

It is interesting to note that Van Dyke and Gordon assume that the shock wave is in the shape of a parabola and that Eq. (3) appears to fit the experimental data closer than their model does at low values of Mach number ($M_1 < 2$). This is probably because at low Mach numbers the shock wave is closer to spherical than parabolic.

References

- Chisnall, R. F., "The Motion of a Shock Wave in a Channel with Applications to Cylindrical and Spherical Shock Waves," *Journal of Fluid Mechanics*, Vol. 2, 1957, pp. 286-298.
- Whitham, G. B., "A New Approach to Problems of Shock Dynamics Part I. Two Dimensional Problems," *Journal of Fluid Mechanics*, Vol. 2, 1957, pp. 145-171.
- Schwartz, R. N. and Eckerman, J., "Shock Location in Front of a Sphere as a Pressure of Neon Gas Effects," *Journal of Applied Physics*, Vol. 27, No. 2, 1956, pp. 169-174.
- Heberle, J. W., Wood, G. P., and Gooderum, P. B., "Data on Shape and Location of Detached Shock Waves on Cones and Spheres," TM 2000, Jan. 1950, NASA.
- Van Dyke, M. D. and Milton, D., "The Supersonic Blunt Body Problem—Review and Extension," *Journal of the Aeronautical Sciences*, Vol. 25, No. 8, 1958, pp. 485-496.
- Van Dyke, M. D. and Gordon, H. D., "Supersonic Flow past a Family of Blunt Axisymmetric Bodies," TR-R-1, 1959, NASA.